Optical bistable devices based on guided-mode resonance in slab waveguide gratings

Quang Minh Ngo[1], Sangin Kim[1*], Seok Ho Song[2], and Robert Magnusson[3]

[1]School of Electrical and Computer Engineering, Ajou University, Suwon 443-749, Korea
[2]Department of Physics, Hanyang University, Seoul 133-791, Korea
[3]Department of Electrical and Computer Engineering, University of Texas, Arlington, TX 76019, USA
sangin@ajou.ac.kr

Abstract: We investigate properties of nonlinear resonant gratings with emphasis on optical bistability. Slab waveguide gratings with various quality factors are designed and their characteristics analyzed with a finite-difference time-domain method. Considerable field enhancements are observed in the gratings and the performance compares favorably with metallic bistable devices. Bistabilitiy based on coupled gratings is also treated. Mechanically controllable switching intensity realized by varying a gap distance between two gratings is demonstrated. Resonant nonlinear elements in this work may find applications in all-optical information processing and optical switching, and our investigation on the dependence of the normalized switching intensity and the response time on quality factor will provide a general guide line for grating-based bistable device design.

OCIS codes: (050.1970) Diffractive optics; (310.2790) Guided waves; (130.1750) Components; (190.1450) Bistability.

References and Links

1. H. M. Gibbs, *Optical bistability*: *Controlling Light with Light* (Academic, 1985).
2. S. F. Mingaleev, and Y. S. Kivshar, "Nonlinear transmission and light localization in photonic-crystal waveguides," J. Opt. Soc. Am. B **19**(9), 2241 (2002).
3. M. Soljacic, M. Ibanescu, S. G. Johnson, Y. Fink, and J. D. Joannopoulos, "Optimal bistable switching in nonlinear photonic crystals," Phys. Rev. E **66**, 055601(R) (2002).
4. M. Soljačić, C. Luo, J. D. Joannopoulos, and S. Fan, "Nonlinear photonic crystal microdevices for optical integration," Opt. Lett. **28**(8), 637–639 (2003).
5. S. Radic, N. George, and G. P. Agrawal, "Optical switching in λ/4-shifted nonlinear periodic structures," Opt. Lett. **19**(21), 1789–1791 (1994).
6. S. Jans, J. He, Z. R. Wasilewski, and M. Cada, "Low threshold optical bistable switching in an asymmetric λ/4-shifted distributed-feedback heterostructures," Appl. Phys. Lett. **67**(8), 1051 (1995).
7. R. Magnusson, and S. S. Wang, "New principle for optical filters," Appl. Phys. Lett. **61**(9), 1022–1024 (1992).
8. Y. Ding, and R. Magnusson, "Resonant leaky-mode spectral-band engineering and device applications," Opt. Express **12**(23), 5661–5674 (2004).
9. R. Magnusson, and M. Shokooh-Saremi, "Physical basis for wideband resonant reflectors," Opt. Express **16**(5), 3456–3462 (2008).
10. K. J. Lee, R. Lacomb, B. Britton, M. Shokooh-Saremi, H. Silva, E. Donkor, Y. Ding, and R. Magnusson, "Silicon-layser guided-mode resonance polarizer with 40-nm bandwidth," IEEE Photon. Technol. Lett. **20**(22), 1857–1859 (2008).
11. D. Wawro, S. Tibuleac, and R. Magnusson, "Optical waveguide-mode resonant biosensors *Optical," Imaging Sensors and Systems for Homeland Security Applications*, (Springer New York, 2006).
12. H. Y. Song, S. Kim, and R. Magnusson, "Tunable guided-mode resonances in coupled gratings," Opt. Express to be published
13. G. Purvinis, P. S. Priambodo, M. Pomerantz, M. Zhou, T. A. Maldonado, and R. Magnusson, "Second-harmonic generation in resonant waveguide gratings incorporating ionic self-assembled monolayer polymer films," Opt. Lett. **29**(10), 1108–1110 (2004).
14. P. Vincent, N. Paraire, M. Neviere, A. Koster, and R. Reinisch, "Grating in nonlinear optics and optical bistability," J. Opt. Soc. Am. B **2**(7), 1106 (1985).
15. I. A. Avrutskii, and V. A. Sychugov, "Optical bistability in an excited nonlinear corrugated waveguide," Sov. J. Quantum. Electron. **20**(7), 856–859 (1990).
16. J. A. Porto, L. Martin-Moreno, and F. J. Garcia-Vidal, "Optical bistability in subwavelength slit apertures containing nonlinear media," Phys. Rev. B **70**, 081402(R) (2004).

#119123 - $15.00 USD Received 27 Oct 2009; revised 1 Dec 2009; accepted 4 Dec 2009; published 7 Dec 2009

17. C. Min, P. Wang, C. Chen, Y. Deng, Y. Lu, H. Ming, T. Ning, Y. Zhou, and G. Yang, "All-optical switching in subwavelength metallic grating structure containing nonlinear optical materials," Opt. Lett. **33**(8), 869–871 (2008).
18. A. Taflove, *Computational Electrodynamics*, (Artech House, Boston, 1995).
19. A. Farjadpour, D. Roundy, A. Rodriguez, M. Ibanescu, P. Bermel, J. D. Joannopoulos, S. G. Johnson, and G. Burr, "Improving accuracy by subpixel smoothing in FDTD," Opt. Lett. **31**, 2972 (2006).
20. H. A. Haus, *Waves and Field in Optoelectronics* (Englewood Cliffs, NJ: Prentice-Hall, 1984).
21. J. M. Laniel, N. Ho, and R. Vallee, "Nonlinear-refractive-index measurement in As_2S_3 channel waveguides by asymmetric self-phase modulation," J. Opt. Soc. Am. B **22**, 437 (2005).
22. I. A. Avrutsky, and V. A. Sychugov, "Reflection of a beam of finite size from a corrugated waveguide," J. Mod. Opt. **36**(11), 1527–1539 (1989).
23. H. B. Liao, R. F. Xiao, H. Wang, K. S. Wong, and G. K. L. Wong, "Large third-order optical nonlinearity in Au:TiO_2 composite films measured on a femtosecond time scale," Appl. Phys. Lett. **72**(15), 1817 (1998).
24. Y. Ding, and R. Magnusson, "MEMS tunable resonant leaky mode filters," IEEE Photon. Technol. Lett. **18**(14), 1479–1481 (2006).

1. Inroduction

Optical bistability is a means to implement all-optical switching and optical memory which are key functions for all-optical information processing applications [1]. Numerous nonlinear materials and optical resonant structures have been studied in the past to realize optical bistable devices. Recently, bistable devices employing nonlinear photonic crystals have been studied [2–4]. They seem to be promising candidates for optical integrated circuit components due to their compact size and reduced operational power. While optical integrated circuits are desired due to their compactness, difficulty in optical fan-in/out may be an obstacle to realization of large scale parallel all-optical signal processors. In this aspect, free-space optics may have an advantage, and bistable devices that can exploit the parallel access scheme have their own significance. Among bistable devices with easy fan-in/out, vertically stacked distributed feedback structures were studied showing low switching intensities with introduction of $\lambda/4$ shift in their periodicity [5,6]. These devices were fabricated using epitaxial growth technology. In this paper, optical bistability in slab waveguide gratings is considered as another possible choice with easy fan-in/out and economic fabrication process. It has been shown that optical filters with versatile spectral attributes can be implemented using guided-mode resonance (GMR) in a thin-film slab waveguide grating [7–11]. The spectral characteristics of coupled gratings can be tuned by nanoelectromechanical actuator technologies [12]. Despite versatile resonance characteristics, nonlinear applications of GMR have not received much attention. Second harmonic generation in a nonlinear thin-film grating has been reported [13]. A feasibility study and theoretical analysis of optical bistable devices based on GMR have been reported previously [14,15]. However, systematic investigation on bistability characteristics, including temporal response, of the nonlinear slab waveguide gratings has not been performed. In this work, optical bistability in slab waveguide gratings is investigated numerically. Field enhancement factors, switching intensities, and temporal response of optical bistable devices based on gratings with various quality factors are analyzed and compared to recently reported results on bistability in subwavelength metal slit array structures [16,17]. Optical bistable devices based on coupled grating are also considered and it is shown that the tunability of coupled gratings enables control of switching intensity by mechanical means. This may be of use in practical all-optical signal processing applications. The calculations in this paper are carried out using the finite-difference time-domain (FDTD) method with subpixel smoothing for increased accuracy [18,19].

2. Bistability in single-grating devices

Figure 1(a) shows a slab waveguide grating structure whose guiding layer is chalcogenide glass (As_2S_3, n = 2.38). The grating is formed by rectangular corrugation, with period (Λ) and filling factor of 780 nm and 0.5, respectively. The glass substrate (refractive index n = 1.5) is assumed to be thick enough with a nonreflecting bottom. Figure 1(b) shows the calculated linear reflection spectra for various grating depths (δ). In the calculation, a transverse-electric (TE) polarized normally incident wave is assumed. A perfectly matched absorbing boundary condition is used for the top and the bottom sides [18]. In the lateral direction, a periodic

#119123 - $15.00 USD Received 27 Oct 2009; revised 1 Dec 2009; accepted 4 Dec 2009; published 7 Dec 2009

boundary condition is applied. As seen in Fig. 1(b), the normally incident wave is resonantly coupled to a leaky waveguide mode and the resulting reflection spectra are close to Lorentzian shape with small background reflection. The waveguide thickness (t) is optimized to reduce the background reflection for each grating depth. For 10 nm < δ < 50 nm, the waveguide thickness of t = 300 nm is found close to an optimal value, and for δ = 90 nm, t = 260 nm is used. As the grating depth decreases, the waveguide mode gets less leaky and hence, the linewidth becomes narrower, that is, quality factor (Q) increases. The characteristics of the GMRs for various grating depths are summarized in Table. 1. Field enhancement factors are also calculated by measuring peak field amplitudes in the waveguides for unit-amplitude incident field in respective gratings.

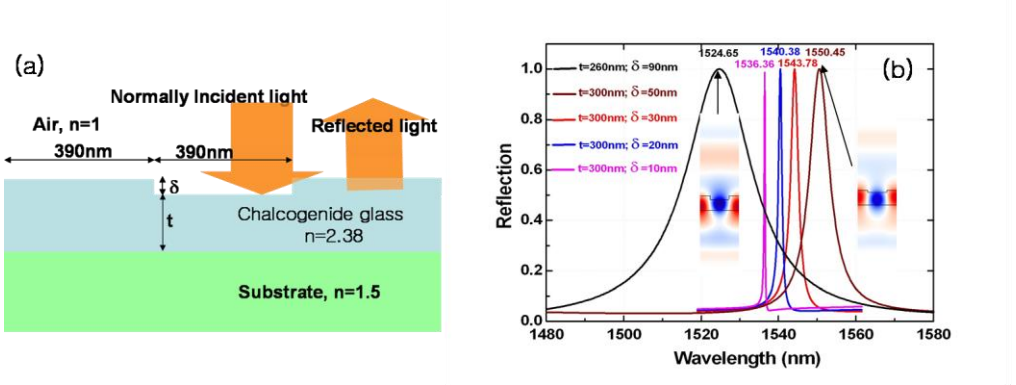

Fig. 1. (a) Slab waveguide grating structure with input light of normal incidence. (b) Reflection spectra for various grating depths (δ). For each grating depth, waveguiding layer thickness is optimized to minimize the background reflection. The insets in (b) show field distributions at resonance. In this example, TE polarized light is used, that is, the electric-field is normal to the incident plane.

Table 1. Characteristics of guided-mode resonances in the example design

Grating depth (nm) (t) (nm)	10 (300)	20 (300)	30 (300)	50 (300)	90 (260)
Center wavelength, λ_o (nm)	1536.36	1540.38	1543.78	1550.45	1524.65
Q-factor	5605	1429	650	248	72
Photon life time, $\tau = Q/\omega_o$ (ps)	4.57	1.17	0.533	0.204	0.0584
Field enhancement factor	53.3	27.0	18.2	11.3	6.4
Minimal grating length or beam size $L=\tau c/n_{eff}$ (μm)	696	178	80.8	30.8	8.97

Based on the linear spectra, operating wavelengths for numerical investigation of optical bistability are determined. To observe bistable behavior, operating frequency (or wavelength) should be detuned from a center frequency according to $(\omega_o-\omega)\tau > \sqrt{3}$, where τ is a photon life time [20]. We choose the operating wavelengths at 20% reflection, which corresponds to a frequency detuning of $(\omega_o-\omega)\tau = 2$ for a Lorentzian spectral shape.

The bistable behavior of the grating is calculated by measuring a reflected flux with an input flux whose magnitude is modulated as a staircase function. A low-reflection flux state is calculated with an increasing staircase function and a high-reflection flux state with a decreasing staircase function. The duration of each stair is kept long enough to get a stable reflection flux. Only the third-order nonlinearity of the chalcogenide glass is considered, and

#119123 - $15.00 USD Received 27 Oct 2009; revised 1 Dec 2009; accepted 4 Dec 2009; published 7 Dec 2009

experimentally measured Kerr nonlinear coefficient of $n_2 = 3.12\text{x}10^{-18}\text{m}^2/\text{W}$ ($\chi^{(3)} = 1.34\text{x}10^{-10}$ esu) is used in the calculation [21]. The time delay of the nonlinear material is ignored. Figure 2 shows the calculated bistable behavior of the gratings with (a) $\delta = 90$ nm, (b) 50 nm, and (c) 10 nm. In all cases, bistable behavior is clearly observed. The transmission through the grating should also show bistability. Figure 2(d) shows the calculated transmission flux in the grating with $\delta = 10$ nm. The contrast ratio between the high and the low states is greatly enhanced. Since transmission at resonance is very close to zero, the low state of the transmission bistability is also very close to zero and hence, high contrast ratio is achievable regardless of the operating wavelength (or frequency) detuning.

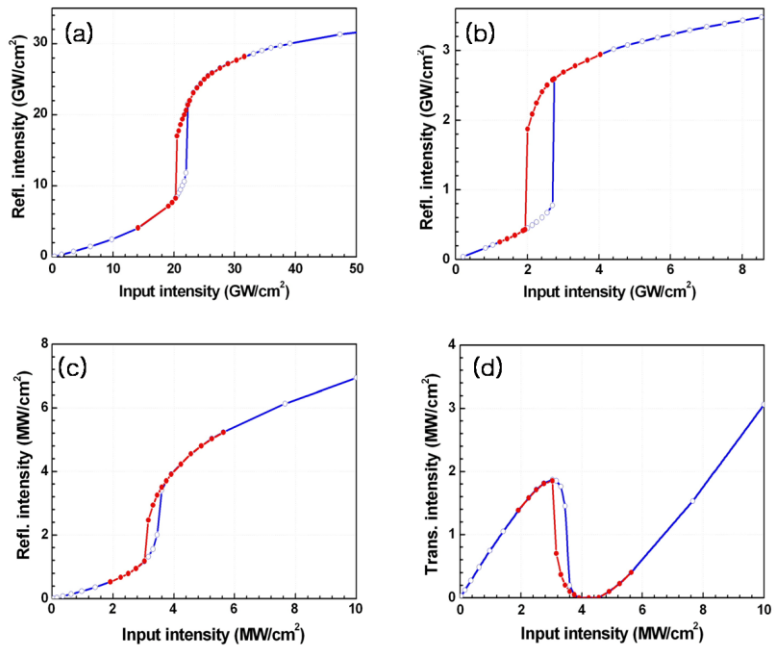

Fig. 2. Bistability in the nonlinear gratings depicted in Fig. 1(a). (a) $\delta = 90$ nm, (b) $\delta = 50$ nm, (c) $\delta = 10$ nm, (d) transmission for $\delta = 10$ nm.

Incident intensities for switching can be estimated from the calculated bistability curves. For example, from Fig. 2, the estimated switching intensities are 22 GW/cm^2, 2.7 GW/cm^2, and 3.4 MW/cm^2, respectively, for the gratings of $\delta = 90$ nm, 50 nm, and 10 nm. The normalized switching incident intensity (in the unit of $1/n_2$) is plotted as a function of quality factor in Fig. 3. The solid (blue) line in Fig. 3 is a fitting line. One can see that the switching intensity is proportional to $1/(Q)^2$, which can be understood in terms of intensity enhancement and spectral linewidth. In Fig. 3, an intensity enhancement factor, which is the square of the field enhancement factor listed in Table 1, is also plotted, and it is proportional to the quality factor of the grating. Note that the solid (red) line is also a fitting line. Since the quality factor is directly proportional to the photon life time ($\tau = Q/\omega_o$), a high quality factor means that the photon remains in the grating longer, and thus, the intensity in the grating is higher for a higher Q. Moreover, a high quality factor implies a narrower linewidth and thus, a smaller amount of resonance spectrum shift is required to change the state. Again, the resonance spectrum shift is directly proportional to the intensity through the refractive index change of the nonlinear material which is governed by $n = n_o + n_2 I$ (or $\varepsilon = \varepsilon_{lin} + \chi^{(3)}|E|^2$). Therefore, the effect of the quality factor on the switching intensity is two-fold, which explains the $1/(Q)^2$ dependency of the switching intensity. Previously, bistability in a metal slit array containing nonlinear material was numerically studied and its normalized switching intensity was about 5

#119123 - $15.00 USD Received 27 Oct 2009; revised 1 Dec 2009; accepted 4 Dec 2009; published 7 Dec 2009

x 10^{-4} [16]. As seen in Fig. 3, the GMR in the nonlinear slab grating shows a normalized intensity smaller than ~1 x 10^{-4} for Q > 250, approximately. In the metal slit, excitation of surface plasmons enhances field strength, but the surface plasmons also suffer from Ohmic loss so that the spectral linewidth broadens for the same external radiative coupling rate ($1/\tau$). The broader linewidth requires higher switching intensity. It seems that this is why the bistability in the slab waveguide grating shows switching intensity comparable to or smaller than that for the metal slit even though the field enhancement may not be as strong as in the metal slit. Therefore, we believe that the slab waveguide grating structure is an alternate candidate for a platform of optical bistable devices with proper nonlinear materials.

The normalized optical intensity in the grating can be estimated by multiplying the normalized incident intensity and the intensity enhancement factor, which is also plotted in the unit of $1/n_2$ in Fig. 3. Obviously, it is proportional to 1/Q and corresponds to the index change needed to switch the state of bistability in the grating, approximately.

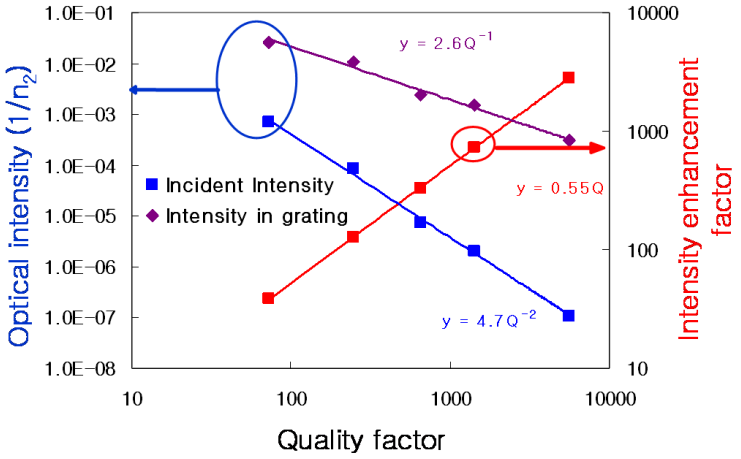

Fig. 3. Optical incident intensity, optical intensity in the grating, and intensity enhancement factor for switching of bistable devices based on gratings of various quality factors. The optical intensity is normalized by ($1/n_2$). The solid lines are fitting curves and their equations are noted.

Switching incident powers can be estimated by multiplying incident beam areas and the switching incident intensities calculated above. It should be noted that the minimal grating length and the minimal beam size in the direction along the incident plane is set by the photon lifetimes and given by $L = \tau c/n_{eff} = Q\lambda_o/n_{eff}$, where c is a speed of light and n_{eff} is an effective index of the waveguide grating. The minimal beam sizes in the direction along the incident plane are estimated for the gratings of various quality factors and listed in Table 1. In the calculation of L, n_{eff} is estimated by $n_{eff} = \lambda_o/\Lambda$. If a grating length or a beam size smaller than L is used, the resonant reflection gets weaker [22], so that the contrast ratio in the resulting optical bistability becomes low. As we use a one-dimensional grating, the beam size in the direction normal to the grating vector does not have a minimal value set by the photon lifetime and can be as small as possible within the diffraction-limit. The incident beam shape does not need to be circular and the beam can be focused as needed by using a cylindrical lens. Therefore, the required minimal beam area can be roughly estimated by $A \approx L\lambda_o = Q\lambda_o^2/n_{eff}$ from a typical spatial resolution of a lens. Consequently, the switching incident power is proportional to 1/Q. The estimated switching power for the gratings of δ = 90 nm, 50 nm, and 10 nm are 3.0 x 10^3 W, 1.3 x 10^3 W, and 36 W, respectively.

Figure 4 shows the calculated temporal response associated with bistability in these gratings. In this example, we set incident intensity above the switching intensity, keep it for a while, and then drop it just below the switching intensity. As seen in Fig. 4, when we turn on the excitation, the reflected intensity shows an overshoot and oscillatory behavior at the

#119123 - $15.00 USD Received 27 Oct 2009; revised 1 Dec 2009; accepted 4 Dec 2009; published 7 Dec 2009

beginning, subsequently stabilizing in time. The rise times are estimated to be 0.2 ps and 15 ps for the gratings of δ = 90 nm and 10 nm, respectively, which correspond to 3.4 x photon life time. When the input intensity is dropped, the reflection followed the upper branch of the bistability curve and remains in the high state. The fall times are about the same as the rise times. The other gratings whose temporal responses are not shown exhibit the same tendency. The dependency of the temporal response on the operating wavelength is also investigated, which reveals that the response time does not show remarkable dependence on the operation wavelength.

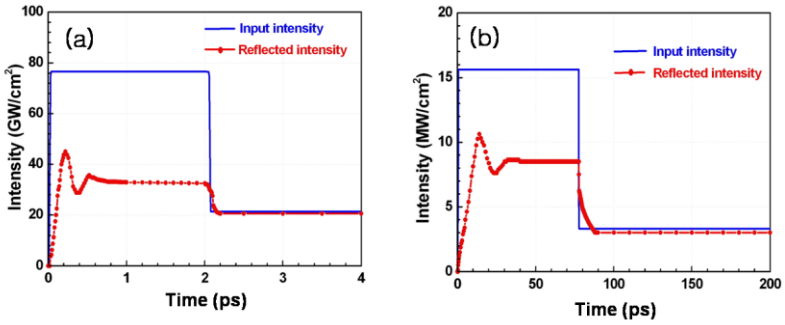

Fig. 4. Temporal response of bistable devices based on gratings of (a) δ = 90 nm and (b) δ = 10 nm.

From the results presented above, we see that there exists a trade-off between the switching optical intensity and the response time, which is a universal tendency in bistable devices based on resonance. To achieve a fast bistable device with a low switching intensity, obviously, material with a large nonlinear coefficient is required. It has been reported that metal-dielectric composite materials such as Au:SiO_2, Au:TiO_2, and Au:Al_2O_3 have high nonlinear susceptibilities $\chi^{(3)} = 10^{-6} \sim 10^{-7}$ esu in the visible region [23], which is 3 ~4 orders of magnitude higher than in As_2S_3. Recently, there was a theoretical study on the bistability in a metal slit array covered with Au:SiO_2 ($\chi^{(3)} = 1.7\text{x}10^{-7}$ esu), which showed a switching intensity of 12MW/cm^2 and a response time of 0.2 ps [17]. Those highly nonlinear composite materials can also be adopted in GMR structures. A slab waveguide grating is designed with Au:TiO_2 (n = 2.4 from Ref [22].) as depicted in Fig. 5(a). The period is 280 nm and the grating depth and the thickness of the guiding layer are 20 nm and 100 nm. The designed GMR has a center wavelength of 555 nm and a quality factor of 183 ($\tau \approx 0.054$ ps) as seen in Fig. 5(b). The bistability shown in Fig. 5(c) and Fig. 5(d) are calculated for the designed GMR structure with the same instantaneous nonlinear susceptibility as used in Ref [17]. ($\chi^{(3)} = 1.7\text{x}10^{-7}$ esu). The operating wavelength is set at 20% reflection. The switching intensity and the response time are approximately 2.2 MW/cm^2 and 0.18 ps, respectively, which is better performance than for the metal slit array. The estimated minimal beam size in the direction along the incident plane is 8.17 μm and the corresponding switching power is approximately 100 mW.

#119123 - $15.00 USD Received 27 Oct 2009; revised 1 Dec 2009; accepted 4 Dec 2009; published 7 Dec 2009

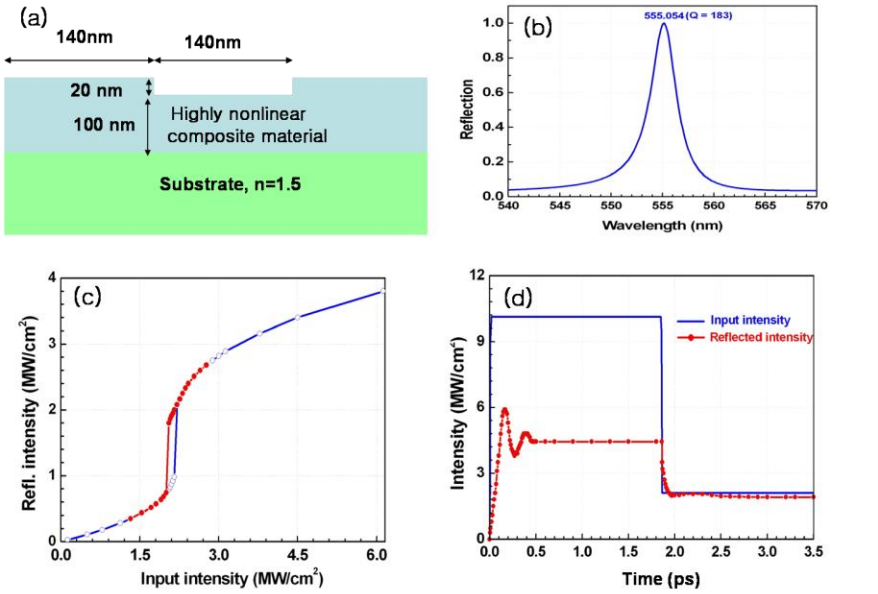

Fig. 5. (a) Slab waveguide grating whose guiding layer is made with a highly nonlinear material (n = 2.4), (b) reflection spectrum, (c) bistability curves, and (d) temporal response.

3. Optical bistability in coupled gratings

As shown in Fig. 3, a dielectric slab waveguide grating can have considerable field enhancement for a large quality factor and the switching intensity decreases as $1/Q^2$. If the switching time is not a limiting factor, a higher quality factor is desired. To achieve a high quality factor, the grating depth can be decreased. Instead of using extremely shallow gratings, if two identical gratings are coupled, an arbitrarily high quality factor can be achieved [12]. Figure 6(a) shows one example, where two gratings of δ = 30 nm considered in the previous section face each other with a gap. When the distance between two gratings is small, two guided modes are evanescently coupled to form super-modes of even and odd symmetries. As a result, additional resonant peaks appear in the reflection spectrum. The linewidth of the peak can be arbitrarily narrow depending on relative phase retardation between the two gratings [12]. Figure 6(b) shows the calculated spectrum for d = 50 nm. Two reflection peaks appear, and one at shorter wavelength has very narrow linewidth ($Q \approx 3 \times 10^4$, τ = 23.3 ps). Note that the quality factor of this peak is ~46 x that of the single grating. Bistability characteristics are calculated for this resonant peak as shown in Fig. 6(c) and Fig. 6(d). The switching intensity is 0.33 MW/cm^2 which corresponds to a normalized intensity of 1.03 x $10^{-8}/n_2$. This is about $(1/27)^2$ times the switching intensity of the single grating and higher than what is expected from the $1/Q^2$ dependence of the switching intensity. In coupled gratings, the field enhancement factor is lower than expected based on the single grating due to the increase of net guiding layer thickness, and this is why the switching intensity is somewhat higher. The estimated minimal beam size in the direction along the incident plane is 3.7 mm and the corresponding switching power is approximately 17.8 W. The response time is 120 ps.

#119123 - $15.00 USD Received 27 Oct 2009; revised 1 Dec 2009; accepted 4 Dec 2009; published 7 Dec 2009

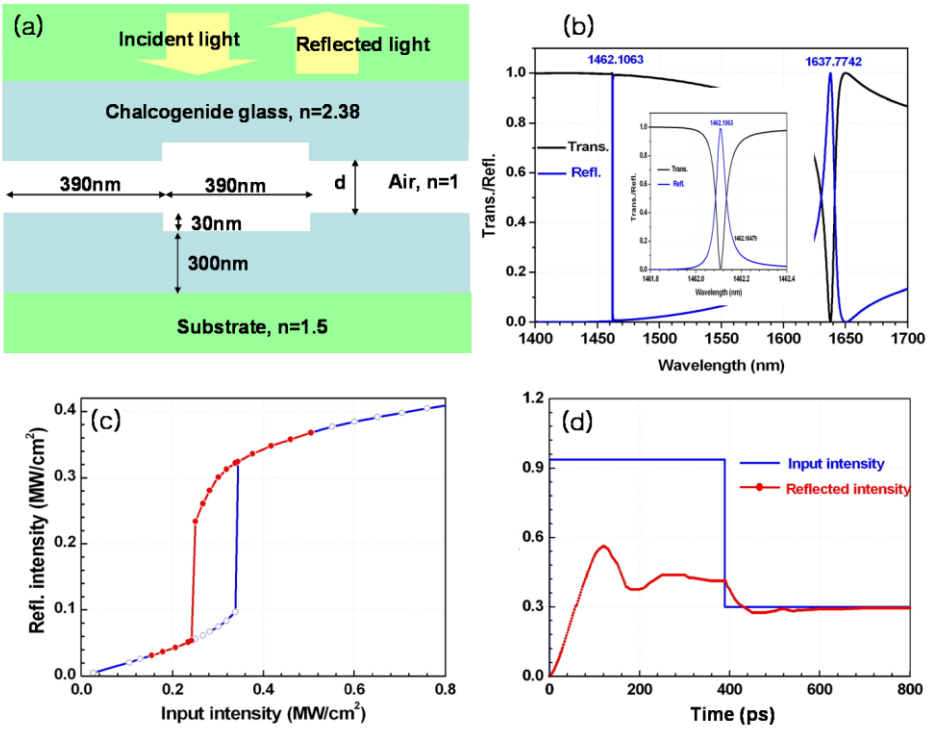

Fig. 6. (a) Coupled identical slab waveguide gratings with a gap of d, (b) reflection spectrum for d = 50nm, (c) bistability curves for d = 50 nm, (d) temporal response for d = 50 nm. The inset in (b) is an enlarged spectrum of the shorter wavelength peak.

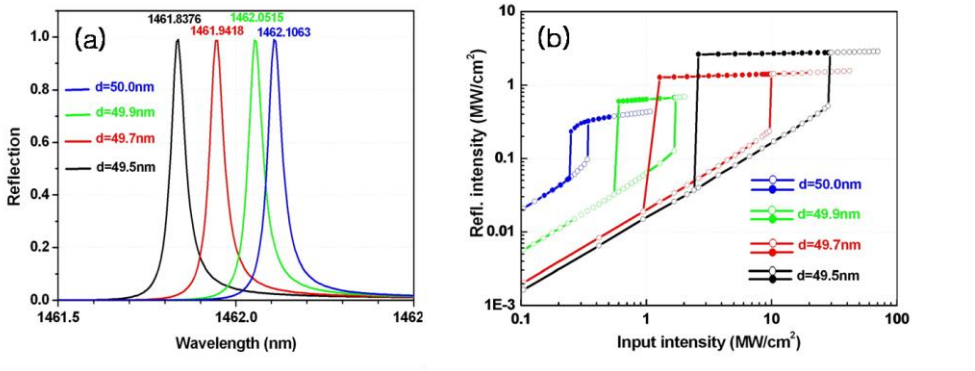

Fig. 7. (a) Reflection spectra and (b) bistability curves of the coupled gratings depicted in Fig. 6(a) for various d. The gap d is varied from 50 to 49.5 nm.

Another useful property of the coupled grating structure is that the resonant wavelength can be tuned mechanically in conjunction with nanoelectromechanical technologies [12,24]. Figure 7(a) shows calculated reflection spectra of the coupled gratings in Fig. 6(a) for various d. Note that only the shorter wavelength peak is shown here. As d varies from 50 nm to 49.5 nm, the center wavelength shifts to the shorter wavelength due to increased evanescent coupling between two resonant modes. Tunable resonance in the coupled gratings can be used to control the switching intensity. For the fixed operating wavelength chosen at 20% reflection position in the spectrum for d = 50 nm, bistabilities curves are calculated for various d as

#119123 - $15.00 USD Received 27 Oct 2009; revised 1 Dec 2009; accepted 4 Dec 2009; published 7 Dec 2009

plotted in Fig. 7(b). As d decreases, more index change is demanded since the spectrum shifts away from the operating wavelength. As a result, the switching intensity increases. This implies that the switching intensity can be controlled mechanically which may be useful in applications since fabrication errors can be compensated. As seen in Fig. 7(b), the switching intensity changed almost by two orders of magnitude for 0.5 nm variation in d. This extreme sensitivity to d variation is relaxed for large d or high quality factor of each grating so that it can be properly designed. The post-fabrication switching intensity control can also be realized by using thermo-optic property of material embedded between the gratings. In this case the extreme sensitivity will require very small amount of temperature change, and it is also possible to design the coupled grating system for further enhanced sensitivity.

4. Conclusion

In this paper, we investigate numerically the bistable behavior of guided-mode resonance in nonlinear slab waveguide gratings. Gratings with various quality factors are designed and their bistability characteristics such as field enhancement, switching intensity, and temporal response are studied systematically. Considerable field enhancement proportional to Q is observed in these elements. The switching intensity shows $1/Q^2$ dependence on quality factor and the response time is $\sim 3.4\tau$. The grating with $Q \approx 5600$ shows a switching intensity of 3.4 MW/cm^2 (corresponding to a normalized switching intensity of $\sim 10^{-7}/n_2$) and a response time of 15 ps. A grating composed of high nonlinear composite material ($\chi^{(3)} = 1.7 \times 10^{-7}$ esu) is also considered, and it shows a switching intensity of 2.2 MW/cm^2 and a response time of 0.18 ps, which is improved performance relative to metal-slit-array-based bistable devices previously reported. Although specific nonlinear materials are assumed in the example gratings considered here, our investigation on the dependence of the normalized switching intensity in the grating and the response time on Q may provide a general guide line for grating-based bistable device design. Optical bistable devices based on coupled gratings are also considered. By coupling two identical chalcogenide glass based gratings of $Q \approx 650$ with a gap of 50 nm, a low switching intensity of 0.33 MW/cm^2 (corresponding to a normalized intensity of $\sim 10^{-8}/n_2$) is obtained. This can be further reduced with a smaller gap. The dependence of the switching intensity on the gap size in the coupled grating is investigated, and almost two orders of magnitude switching intensity change for 0.5 nm gap size variation at d = 50 nm is demonstrated. This extreme sensitivity can be relaxed or enhanced by properly designing the coupled grating system.

Acknowledgement

This work was supported by National Research Foundation of Korea Grant (KRF-2009-0058569), the Korea Research Foundation Grant (KRF-2007-412-J04002), and the Korea Science and Engineering Foundation grant (R11-2008-095-01000-0) funded by the Korean Government (MEST). This material is also based, in part, upon work supported by the National Science Foundation under Grant No. ECCS-0702307 and by the Texas Nanoelectronics Research Superiority Award funded by The Texas Emerging Technology Fund.

#119123 - $15.00 USD Received 27 Oct 2009; revised 1 Dec 2009; accepted 4 Dec 2009; published 7 Dec 2009